A stepped-impedance bandstop filter with extended upper passbands and improved pass-band reflections

Xiaoying Zuo and Jianguo Yu

Citation: AIP Advances **6**, 095106 (2016); doi: 10.1063/1.4962668
View online: http://dx.doi.org/10.1063/1.4962668
View Table of Contents: http://aip.scitation.org/toc/adv/6/9
Published by the American Institute of Physics

A stepped-impedance bandstop filter with extended upper passbands and improved pass-band reflections

Xiaoying Zuo[a] and Jianguo Yu
School of Electronic Engineering, Beijing University of Posts and Telecommunications, P.O. Box. 282, Beijing 100876, China

(Received 1 July 2016; accepted 31 August 2016; published online 8 September 2016)

A high-performance planar bandstop filter with extended upper passbands and improved pass-band return loss is proposed in this article. In this proposed band-stop filter, a novel three-section stepped-impedance structure is suggested to improve the pass-band reflections without affecting the desired band-stop and extended upper passband performances. The analysis and design considerations of this filter are provided while the proposed design approach is verified by full-wave simulation, microstrip implementation and accurate measurement of a typical fabricated filter operating at 1 GHz(f_o). Compared to the conventional one, the proposed band-stop filter has main and obvious advantages of simple single-layer structure, perfect band-stop filtering performance (Suppression of better than 20 dB), excellent low/high pass-band return loss (Reflection of lower than -17 dB) in the extended upper passbands(Larger than 5.96 f_o), and flat group-delay transmission (Variations of smaller than 0.22 ns). [http://dx.doi.org/10.1063/1.4962668]

I. INTRODUCTION

In advanced multi-function radio-frequency/microwave transceivers, bandstop filters with different performances have been widely applied to reject the unwanted frequencies without affecting the desired frequencies.[1,2] Recently, various performances of bandstop filters have been investigated, such as dual/mutli-band operations,[3,4] size reduction,[5] and upper-passband extension.[6] As an ideal bandstop fitler, it is always expected that the bandstop performance occurs only at the desired frequencies while the low insertion-loss passband locates at other pass frequency bands. However, due to periodic characteristics of transmission-line stubs, the odd-number harmonics have bandstop performance in conventional bandstop filters.[1] Since the first upper-passband extension technology has been proposed in Ref. 6, many improvements of bandstop filters with wide upper passbands have been researched in Refs. 7–10. However, the pass-band features in Refs. 7–10 are not perfect when a single-section configuration is considered. Usually, the reflection coefficients in pass bands are larger than -15 dB, even -10 dB in some special cases. Recently, novel technologies including the minimum through-line length,[11] hybrid microstrip/CPW-DGS with via-hole connection,[12] and dual-coupled resonators[13] are proposed to design narrow-band or wide-band bandstop filters. However, the upper pass-band bandwidths in Refs. 11–13 are very narrow, indicating the limited upper pass band.

In order to improve the pass-band performance of bandstop filters with maintaining wide upper passband bandwidth in a single structure, a novel three-section stepped-impedance structure is proposed in a new high-performance planar bandstop filter. The parameter analysis and design considerations of this proposed filter are provided while the proposed design approach is verified by full-wave simulation, microstrip implementation and accurate measurement of a typical fabricated filter operating at 1 GHz (f_o). Compared to the conventional one, the main and obvious advantages of this proposed bandstop filter include a simple single-layer structure, perfect band-stop filtering

[a]E-mail: zuoxiaoying03@163.com

performance (suppression of better than 20 dB), excellent low/high pass-band return loss (reflection of lower than -17 dB) in the extended upper passbands (larger than 5.96 f_o), and flat group-delay transmission (variations of smaller than 0.22 ns).

II. CIRCUIT CONFIGURATION AND DESIGN THEORY OF THE PROPOSED BANDSTOP FILTER

In order to illustrate the novel design concept and optimization process of the proposed bandstop filter, a general Pi-type circuit network model with completely defined circuit parameters is shown in Figure 1(a). According to the typical bandstop filter without performance enhancement,[1] a uniform transmission line and two 90-degree open stubs are used to construct the simplest bandstop filter, as shown in Figure 1(b). To achieve enhanced upper passbands, an improved bandstop filter with stepped-impedance stubs is developed in Refs. 6,7 while the corresponding circuit configuration is presented in Figure 1(c). In general, a high-performance planar bandstop filter should have extended upper passbands and improved pass-band return loss, simultaneously. In this proposed bandstop filter, as shown in Figure 1(d), a novel three-section stepped-impedance structure is proposed to improve the pass-band reflections without affecting the desired band-stop and extended upper passband performances.

The scattering parameters of two-port general network model in Figure 1(a) can be calculated by

$$S^i_{11\mathrm{F}}(f) = \frac{A^i_{\mathrm{F}}(f)R_0 + B^i_{\mathrm{F}}(f) - C^i_{\mathrm{F}}(f)R_0^2 - D^i_{\mathrm{F}}(f)R_0}{A^i_{\mathrm{F}}(f)R_0 + B^i_{\mathrm{F}}(f) + C^i_{\mathrm{F}}(f)R_0^2 + D^i_{\mathrm{F}}(f)R_0}, \tag{1}$$

$$S^i_{21\mathrm{F}}(f) = \frac{2R_0}{A^i_{\mathrm{F}}(f)R_0 + B^i_{\mathrm{F}}(f) + C^i_{\mathrm{F}}(f)R_0^2 + D^i_{\mathrm{F}}(f)R_0}, \tag{2}$$

where

$$\begin{bmatrix} A^i_{\mathrm{F}}(f) & B^i_{\mathrm{F}}(f) \\ C^i_{\mathrm{F}}(f) & D^i_{\mathrm{F}}(f) \end{bmatrix} = \begin{bmatrix} 1 & 0 \\ K^i_{\mathrm{T}}(f) & 1 \end{bmatrix} \begin{bmatrix} A^i_{\mathrm{T}}(f) & B^i_{\mathrm{T}}(f) \\ C^i_{\mathrm{T}}(f) & D^i_{\mathrm{T}}(f) \end{bmatrix} \begin{bmatrix} 1 & 0 \\ K^i_{\mathrm{T}}(f) & 1 \end{bmatrix}, \tag{3}$$

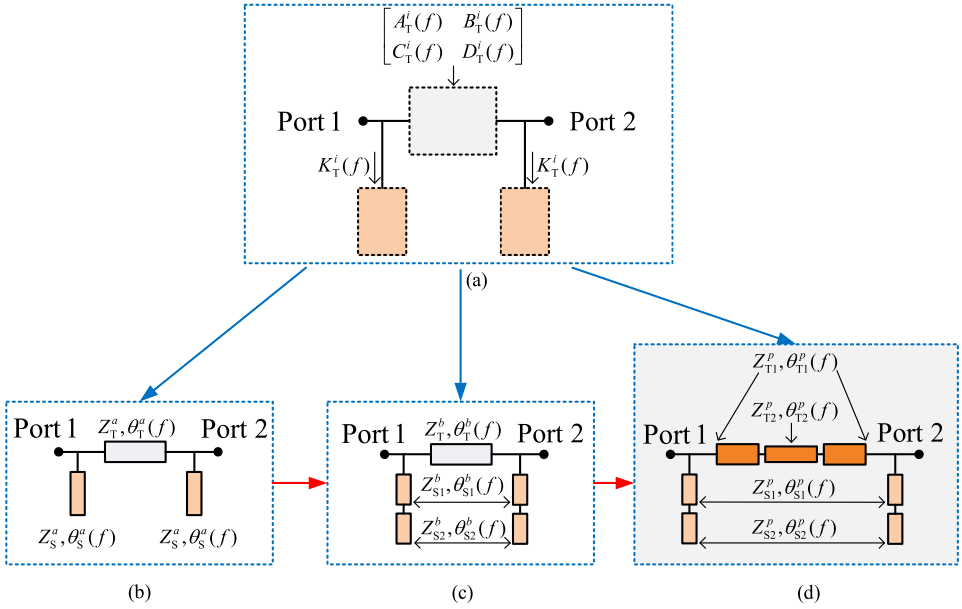

FIG. 1. The **general** network model and circuit parameters (a) of general Pi-type filters, (b) the **conventional** bandstop filter with narrow upper passband (Type I),[1] (c) the **improved** bandstop filter with wide upper passband (Type II),[6,7] (d) the **proposed** bandstop filter with extended upper passbands and improved pass-band reflections.

and R_0 is defined as the port impedance of the filters.[1] In theory, three types of bandstop filters are based on the general network model in Figure 1(a). For the simplest bandstop filter (Type I, $i = 1$) in Figure 1(b), the circuit parameters are given by

$$K_{\mathrm{T}}^{i}(f)_{(i=1)} = \frac{j\tan[\theta_{\mathrm{S}}^{a}(f)]}{Z_{\mathrm{S}}^{a}}, \tag{4}$$

$$\begin{bmatrix} A_{\mathrm{T}}^{i}(f)_{(i=1)} & B_{\mathrm{T}}^{i}(f)_{(i=1)} \\ C_{\mathrm{T}}^{i}(f)_{(i=1)} & D_{\mathrm{T}}^{i}(f)_{(i=1)} \end{bmatrix} = \begin{bmatrix} \cos[\theta_{\mathrm{T}}^{a}(f)] & jZ_{\mathrm{T}}^{a}\sin[\theta_{\mathrm{T}}^{a}(f)] \\ \frac{j\sin[\theta_{\mathrm{T}}^{a}(f)]}{Z_{\mathrm{T}}^{a}} & \cos[\theta_{\mathrm{T}}^{a}(f)] \end{bmatrix}. \tag{5}$$

For the improved bandstop filter (Type II, $i = 2$,[6,7]) shown in Figure 1(c), the circuit parameters can be expressed as

$$K_{\mathrm{T}}^{i}(f)_{(i=2)} = j\frac{Z_{\mathrm{S1}}^{b}\tan[\theta_{\mathrm{S2}}^{b}(f)] + Z_{\mathrm{S2}}^{b}\tan[\theta_{\mathrm{S1}}^{b}(f)]}{Z_{\mathrm{S1}}^{b}Z_{\mathrm{S2}}^{b} - Z_{\mathrm{S1}}^{b}Z_{\mathrm{S1}}^{b}\tan[\theta_{\mathrm{S1}}^{b}(f)]\tan[\theta_{\mathrm{S2}}^{b}(f)]}, \tag{6}$$

$$\begin{bmatrix} A_{\mathrm{T}}^{i}(f)_{(i=2)} & B_{\mathrm{T}}^{i}(f)_{(i=2)} \\ C_{\mathrm{T}}^{i}(f)_{(i=2)} & D_{\mathrm{T}}^{i}(f)_{(i=2)} \end{bmatrix} = \begin{bmatrix} \cos[\theta_{\mathrm{T}}^{b}(f)] & jZ_{\mathrm{T}}^{b}\sin[\theta_{\mathrm{T}}^{b}(f)] \\ \frac{j\sin[\theta_{\mathrm{T}}^{b}(f)]}{Z_{\mathrm{T}}^{b}} & \cos[\theta_{\mathrm{T}}^{b}(f)] \end{bmatrix}. \tag{7}$$

When three-section stepped-impedance structure is proposed in this paper, as shown in Figure 1(d), a new type (Type III, $i = 3$) high-performance bandstop filter is constructed. Its circuit parameters have been provided by

$$K_{\mathrm{T}}^{i}(f)_{(i=3)} = j\frac{Z_{\mathrm{S1}}^{p}\tan[\theta_{\mathrm{S2}}^{p}(f)] + Z_{\mathrm{S2}}^{p}\tan[\theta_{\mathrm{S1}}^{p}(f)]}{Z_{\mathrm{S1}}^{p}Z_{\mathrm{S2}}^{p} - Z_{\mathrm{S1}}^{p}Z_{\mathrm{S1}}^{p}\tan[\theta_{\mathrm{S1}}^{p}(f)]\tan[\theta_{\mathrm{S2}}^{p}(f)]}, \tag{8}$$

$$\begin{bmatrix} A_{\mathrm{T}}^{i}(f)_{(i=3)} & B_{\mathrm{T}}^{i}(f)_{(i=3)} \\ C_{\mathrm{T}}^{i}(f)_{(i=3)} & D_{\mathrm{T}}^{i}(f)_{(i=3)} \end{bmatrix} = \begin{bmatrix} \cos[\theta_{\mathrm{T1}}^{p}(f)] & jZ_{\mathrm{T1}}^{p}\sin[\theta_{\mathrm{T1}}^{p}(f)] \\ \frac{j\sin[\theta_{\mathrm{T1}}^{p}(f)]}{Z_{\mathrm{T1}}^{p}} & \cos[\theta_{\mathrm{T1}}^{p}(f)] \end{bmatrix} \begin{bmatrix} \cos[\theta_{\mathrm{T2}}^{p}(f)] & jZ_{\mathrm{T2}}^{p}\sin[\theta_{\mathrm{T2}}^{p}(f)] \\ \frac{j\sin[\theta_{\mathrm{T2}}^{p}(f)]}{Z_{\mathrm{T2}}^{p}} & \cos[\theta_{\mathrm{T2}}^{p}(f)] \end{bmatrix} \begin{bmatrix} \cos[\theta_{\mathrm{T1}}^{p}(f)] & jZ_{\mathrm{T1}}^{p}\sin[\theta_{\mathrm{T1}}^{p}(f)] \\ \frac{j\sin[\theta_{\mathrm{T1}}^{p}(f)]}{Z_{\mathrm{T1}}^{p}} & \cos[\theta_{\mathrm{T1}}^{p}(f)] \end{bmatrix}. \tag{9}$$

In the above equations (1)-(9), the frequency f can be considered as a controllable variable for different operating bands. In the design process, this frequency f can be chosen as the center frequency of the bandstop filters, namely, f_0. For ease of theoretical explanations and examples verifications, we choose $f_0 = 1$ GHz for all examples of bandstop filters.

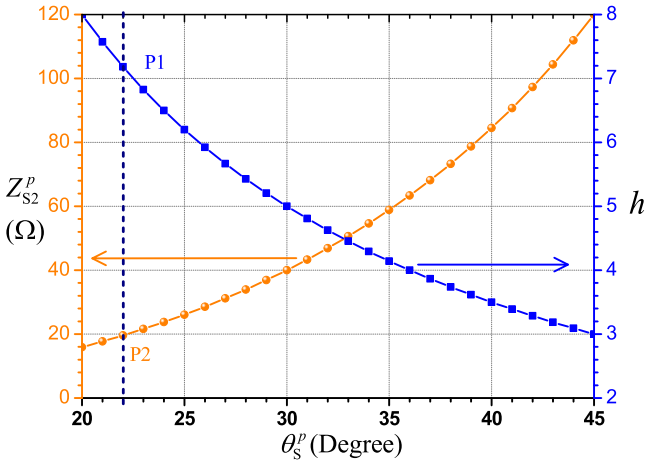

FIG. 2. The practical impedance Z_{S2}^{p} and frequency ratio h versus electrical length θ_{S}^{p}.

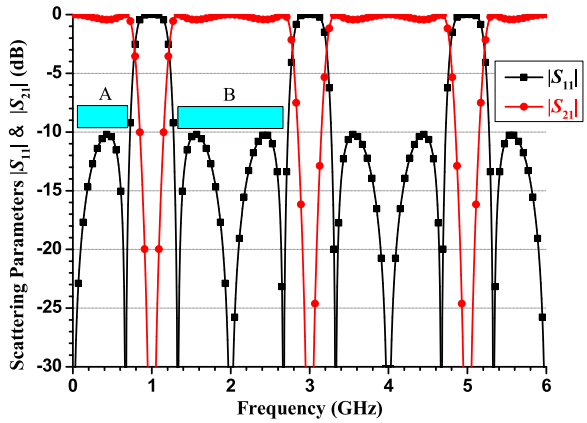

(a)

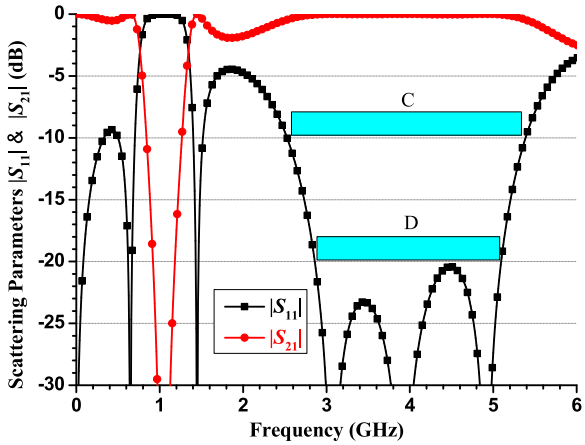

(b)

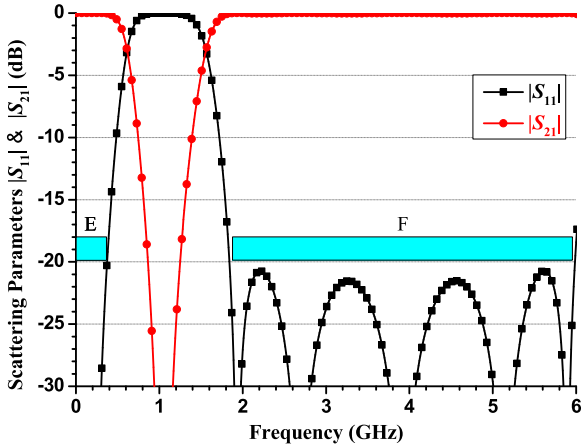

(c)

FIG. 3. The calculated scattering parameters of three types of bandstop filters: (a) Type-I bandstop filter, (b) Type-II bandstop filter, and (c) Type-III bandstop filter (**Proposed**).

It can be found that the bandstop frequency occurs when the condition $K_{\mathrm{T}}^{i}(f_0) = \infty$ is satisfied. Using (8) and the condition $K_{\mathrm{T}}^{i}(f_0) = \infty$, we can obtain a simple equation as

$$Z_{\mathrm{S2}}^{p} = Z_{\mathrm{S1}}^{p} \tan[\theta_{\mathrm{S1}}^{p}(f_0)] \tan[\theta_{\mathrm{S2}}^{p}(f_0)]. \tag{10}$$

In addition, when the first upper external bandstop frequency f_1 occurs and $\theta^p_S(f) = \theta^p_{S1}(f) = \theta^p_{S2}(f)$ is considered, the equation (10) is also satisfied and the following relationship should be assured:

$$\tan^2[\theta^p_S(f_0)] = \tan^2[\theta^p_S(f_1)]. \tag{11}$$

Here, based on (10) and (11), we can obtain the final mathematical expression for f_1:

$$f_1 = \frac{180^o}{\theta^p_S(f_0)} - f_0. \tag{12}$$

In practical microstrip implementation, the common highest available value of characteristic impedance is 120 Ω. Therefore, we choose $Z^p_{S1} = 120\,\Omega$. When different electrical lengths θ^p_S at f_0 are used, the corresponding practical impedance Z^p_{S2} and frequency ratio $h = f_1/f_0$ are presented in Figure 2. When $\theta^p_S(f_0) = 22^o$, the value of Z^p_{S2} is approximately equal to 19.6 Ω and the frequency ratio h is approximately equal to 7.18. This information is located in the points P1 and P2 in the Figure 2. In this special case, the frequency ratio h is the largest and the electrical length θ^p_S is the shortest when the lowest available value of characteristic impedance is limited by 19.6 Ω, indicating the widest available upper passband of the proposed bandstop filters.

Next, three typical calculated examples are designed for three different types of bandstop filters. In the first bandstop filter (Type I), the circuit parameters are $Z^a_T = 50\,\Omega$, $\theta^a_T(f_0) = 90^o$, $Z^a_S = 76\,\Omega$, and $\theta^a_S(f_0) = 90^o$. The scattering parameters $S_{11} = S^{i=1}_{11F}(f)$ and $S_{21} = S^{i=1}_{21F}(f)$ are shown in Figure 3(a). In the Type I bandstop filer, the bandstop performance occurs at both 3 GHz and 6 GHz, and the upper passband B in Figure 3(a) is not very wide. In the second bandstop filter (Type II), the circuit parameters are $Z^b_T = 50\,\Omega$, $\theta^b_T(f_0) = 90^o$, $Z^b_{S1} = 100\,\Omega$, $\theta^b_{S1}(f_0) = 23^o$, $Z^b_{S2} = 20\,\Omega$, and $\theta^b_{S2}(f_0) = 23^o$. The scattering parameters $S_{11} = S^{i=2}_{11F}(f)$ and $S_{21} = S^{i=2}_{21F}(f)$ are shown in Figure 3(b). It can be observed that the upper passband outside of C and D in Figure 3(b) is not perfect and the insertion loss is high. In the final proposed bandstop filter (Type III), the circuit parameters are $Z^p_{T1} = 68\,\Omega$, $\theta^p_{T1}(f_0) = 23^o$, $Z^p_{T2} = 120\,\Omega$, $\theta^p_{T2}(f_0) = 46^o$, $Z^p_{S1} = 100\,\Omega$, $\theta^p_{S1}(f_0) = 23^o$, $Z^p_{S2} = 20\,\Omega$, and $\theta^p_{S2}(f_0) = 23^o$. The scattering parameters $S_{11} = S^{i=3}_{11F}(f)$ and $S_{21} = S^{i=3}_{21F}(f)$ are shown in Figure 3(c). It is very obvious in Figure 3(c) that the reflection coefficients are lower than -20 dB in both the low passband E and high passband F.

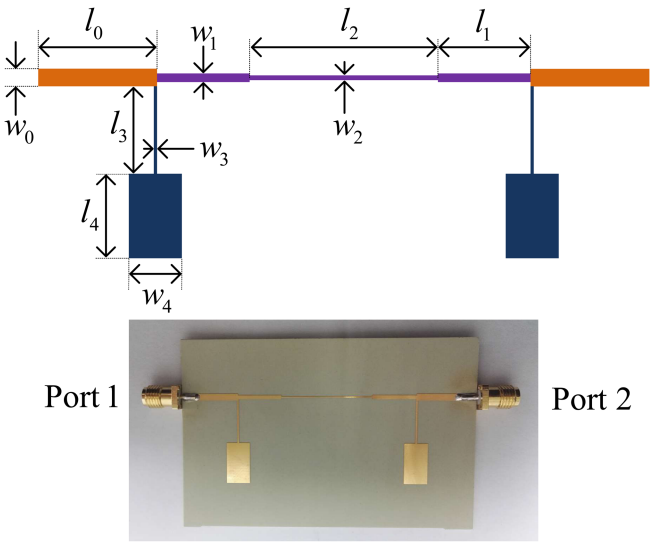

FIG. 4. The layout of the fabricated bandstop filter with physical dimensions and the photograph of the practical circuit.

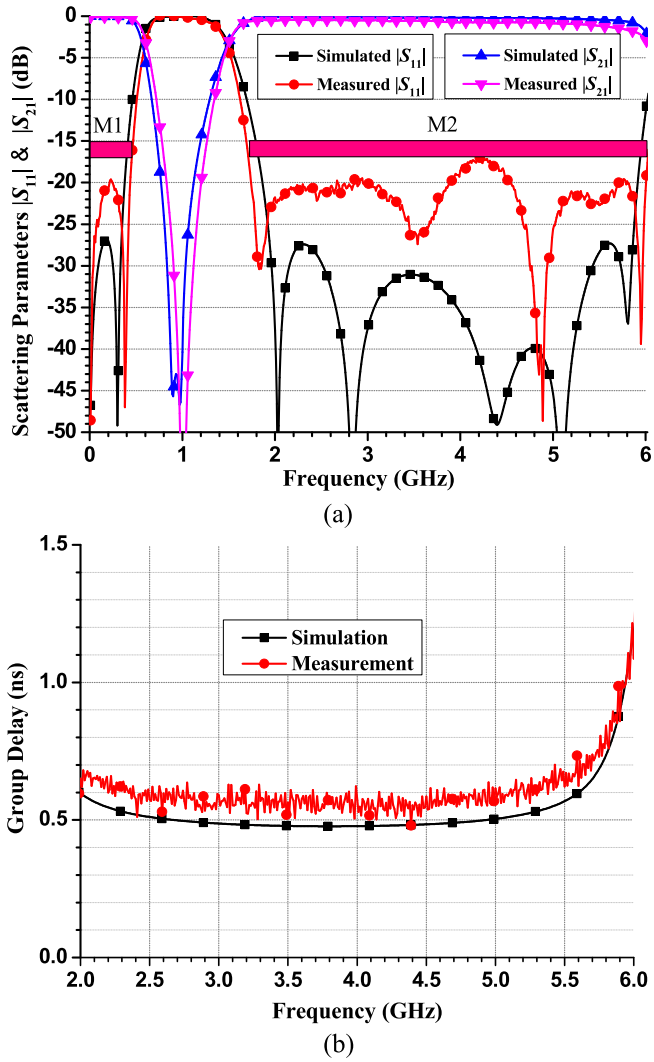

FIG. 5. The simulated and measured results of the fabricated bandstop filter. (a) scattering parameters, and (b) group delay.

It is very interesting that the highest pass-band frequency of the area F is almost equal to 5.98 GHz (h = 5.98).

Finally, for clearly presenting the design steps and conveniently following this proposed research approach for readers or engineers, a simple design procedure in details is summarized as follows:

1) According to the special requirements in practical research projects, set the operating frequency f_0 and the desired frequency ratio h under the limitations shown in Figure 2.
2) Based on the circuit structure shown in Figure 1(d) and the analyzed equations (1-3, 8-10), choose proper circuit parameters to obtain the desired pass-band return loss and bandstop performances. One typical case of the common optimum circuit parameters and ideally calculated scattering parameters are given in Figure 3(c). If the designers want to neglect the optimization process, please directly choose the given Type-III example in Figure 3(c).
3) Transform the ideal transmission lines to practical lines, such as microstrip and CPW, by using a chosen substrate with the known relative permittivity, thickness, and loss tangent.
4) Carefully tune the final circuit layout and full-wave simulation results to satisfy the final requirements.

TABLE I. Performance Comparison of Bandstop Filters.

Refs.	Operating Frequency	Bandstop Bandwidth ($\|S_{21}\|$<-20 dB)	Low Pass Band ($\|S_{11}\|$<-17 dB)	Upper Pass Band ($\|S_{11}\|$<-17 dB)	Matching Technologies
7	≈ 2 GHz	≈ 12.5%	⊗[e]	3.5~9 GHz (h ≈ 4.5)	UL[a]
8	≈ 1 GHz	≈ 30 %	⊗[e]	⊗[e]	Three-Line CLs[b]
9	0.46 GHz	≈ 25 %	⊗[e]	⊗[e]	Two-Line CLs[c]
11	≈ 3.0 GHz	≈ 1.5 %	0.5~2.96 GHz	3.04~3.6 GHz (h ≈ 1.2)	Non-Resonating Node
12	5.44 GHz	35.5%	0.2~4.0 GHz	⊗[e]	UL[a]
13	0.5 GHz	≈ 7 %	0~0.47 GHz	0.65~0.95 GHz (h ≈ 1.9)	Short-Through Line
This work	**1.01 GHz**	**36.45%**	**0~0.45 GHz**	**1.72~6.02 GHz (h=5.96)**	**Three-Section SIS[d]**

[a]Uniform Line (UL).
[b]Three-Line Coupled Lines (CLs).
[c]Two-Line Coupled Lines (CLs).
[d]Three-Section Stepped-Impedance Structure (SIS).
[e]⊗: Unavailable.

III. FULL-WAVE SIMULATION AND EXPERIMENTAL MEASUREMENT OF THE FABRICATED BANDSTOP FILTER

As an experimental verification for this proposed bandstop filter, a microstrip example operating at 1 GHz is designed, simulated, and measured by using a Rogers 4350B substrate of the relative permittivity of $\varepsilon_r = 3.48$, the thickness of h=0.762 mm and the loss tangent of 0.0037. The planar circuit layout with defined physical dimensions and the fabricated bandstop filter are demonstrated in Figure 4. The accurate values of physical dimensions are w_0 = 1.66 mm, w_1 = 0.89 mm, w_2 = 0.206 mm, w_3 = 0.31 mm, w_4 = 6.1 mm, l_0 = 15 mm, l_1 = 11.57 mm, l_2 = 24 mm, l_3 = 11.87 mm, and l_4 = 10.73 mm.

Figure 5(a) shows the simulated and measured scattering parameters. The measured 20-dB insertion-loss ($|S_{21}|$<-20 dB) bandstop bandwidth is from 0.83 GHz to 1.20 GHz (the fractional bandwidth is 36.45%). When the 17-dB return-loss ($|S_{11}|$<-17 dB) limitation is considered for defining the measured pass-band bandwidth, the available low pass band is from DC to 0.45 GHz (M1) and the upper one is from 1.72 GHz to 6.02 GHz (M2). The measured center frequency of the bandstop band is 1.01 GHz and the highest -17-dB reflection-coefficient upper pass-band frequency is 6.02 GHz, indicating $f_1 = hf_0 = 5.96\, f_0$. In general, there is a good agreement between simulated and measured results in Figure 5(a). Figure 5(b) shows the simulated and measured group delays of upper pass band (2~6 GHz). It can be observed that the measured group delay in the band of 2.0 to 5.5 GHz is almost 0.59 ± 0.11 ns.

In order to highlight the advantages of this proposed bandstop filter, the performance comparison between the proposed filters and other published filters is listed in Table I.

IV. CONCLUSIONS

A novel planar bandstop filter with a simple structure and optimum parameters is proposed in this paper. The two main advantages of this bandstop filter are very wide upper passband (the maximum upper frequency ratio is near 6) and practically acceptable return-loss (larger than 17 dB) in both low and upper pass bands. The total design theory and performance predication have been verified by microstrip implementations. It can be expected that this proposed high-performance bandstop filter will be used or integrated in radio-frequency/microwave/millimeter-wave transceivers or other types of systems.

ACKNOWLEDGMENTS

This work was supported by National Natural Science Foundations of China (No. 61372035, and No. 61531007).

[1] J. S. Hong and M. J. Lancaster, *Microstrip Filters for RF/Microwave Applications*, Wiley-Interscience Publication, Chapters 2 and 6, 2001, pp.7–190.
[2] R. V. Snyder, A. Mortazawi, I. Hunter, S. Bastioli, G. Macchiarella, and K. Wu, "Present and future trends in filters and multiplexers," IEEE Transactions on Microwave Theory and Techniques **63**, 3324–3360 (2015).
[3] K. Chin, J. Yeh, and S. Chao, "Compact dual-band bandstop filters using stepped-impedance resonators," IEEE Microwave and Wireless Components Letters **17**, 849–851 (2007).
[4] K. Adhikari and N. Kim, "A miniaturized quad-band bandstop filter with high selectivity based on shunt-connected, T-shaped stub-loaded, stepped-impedance resonators," Microwave and Optical Technology Letters **57**, 1129–1132 (2015).
[5] D. La, W. Han, and J. Zhang, "Compact band-stop filters using Pi-shape DGS and Pi-shape DMS," Microwave and Optical Technology Letters **56**, 2504–2507 (2014).
[6] R. Levy, R. V. Snyder, and S. Shin, "Bandstop filters with extended upper passbands," IEEE Transactions on Microwave Theory and Techniques **54**, 2503–2515 (2006).
[7] M. A. S. Alkanhal, "Compact bandstop filters with extended upper passbands," Active and Passive Electronic Components **2008**, 1–6, Article ID 356049.
[8] W. Tang and J. S. Hong, "Coupled stepped-impedance-resonator bandstop filter," IET Microwaves, Antennas & Propagation **4**, 1283–1289 (2010).
[9] Y. Wu and Y. Liu, "A coupled-line band-stop filter with three-section transmission-line stubs and wide upper pass-band performance," Progress In Electromagnetics Research **119**, 407–421 (2011).
[10] W. M. Fathelbab, "Two novel classes of band-reject filters realizing broad upper pass bandwidth-synthesis and design," IEEE Transactions on Microwave Theory and Techniques **59**, 250–259 (2011).
[11] E. J. Naglich and A. C. Guyette, "Reflection-mode bandstop filters with minimum through-line length," IEEE Transactions on Microwave Theory and Techniques **63**, 3479–3486 (2015).
[12] H. Chen, D. Jiang, and X. Chen, "Wideband bandstop filter using hybrid microstrip/CPW-DGS with via-hole connection," Electronics Letters **52**, 1469–1470 (2016).
[13] A. C. Guyette and E. J. Naglich, "Short-through-line bandstop filters using dual-coupled resonators," IEEE Transactions on Microwave Theory and Techniques **64**, 459–466 (2016).